

# Random projections in gravitational wave searches of compact binaries

Sumeet Kulkarni,<sup>1</sup> Khun Sang Phukon,<sup>2</sup> Amit Reza,<sup>3</sup> Sukanta Bose,<sup>4,5</sup>

Anirban Dasgupta,<sup>3</sup> Dilip Krishnaswamy,<sup>6</sup> and Anand S. Sengupta<sup>3</sup>

<sup>1</sup>*Department of Physics, Indian Institute of Science Education and Research, Homi Bhabha Road, Pune 411008, India.*

<sup>2</sup>*Department of Physics, Indian Institute of Technology, Kanpur 208016, India.*

<sup>3</sup>*Indian Institute of Technology Gandhinagar, Gujarat 382355, India.*

<sup>4</sup>*Inter-University Centre for Astronomy and Astrophysics, Post Bag 4, Ganeshkhind, Pune 411 007, India*

<sup>5</sup>*Department of Physics & Astronomy, Washington State University, 1245 Webster, Pullman, WA 99164-2814, U.S.A*

<sup>6</sup>*IBM Research, Bangalore 560045, India.*

Random projection (RP) is a powerful dimension reduction technique widely used in analysis of high dimensional data. We demonstrate how this technique can be used to improve the computational efficiency of gravitational wave searches from compact binaries of neutron stars or black holes. Improvements in low-frequency response and bandwidth due to detector hardware upgrades pose a data analysis challenge in the advanced LIGO era as they result in increased redundancy in template databases and longer templates due to higher number of signal cycles in band. The RP-based methods presented here address both these issues within the same broad framework. We first use RP for an efficient, singular value decomposition inspired template matrix factorization and develop a geometric intuition for why this approach works. We then use RP to calculate approximate time-domain correlations in a lower dimensional vector space. For searches over parameters corresponding to non-spinning binaries with a neutron star and a black hole, a combination of the two methods can reduce the total on-line computational cost by an order of magnitude over a nominal baseline. This can, in turn, help free-up computational resources needed to go beyond current spin-aligned searches to more complex ones involving generically spinning waveforms. (Preprint number: [LIGO-P1700443-v2](#).)

**Introduction.** The direct detections of gravitational waves (GWs) from the mergers of binary black holes (BBHs) by Advanced LIGO (aLIGO) [1] detectors in the first and second observing runs (O1 and O2, respectively) have launched the era of GW astronomy [2–6]. Recently, Advanced Virgo (AdV) [7] joined aLIGO in detecting GW signals from BBHs [8, 9] and a binary neutron star (BNS) merger [10]. The transient GW signal from the latter was associated with a gamma-ray burst [11] and multiple electromagnetic counterparts [12]. In the coming years, additional ground-based detectors, such as KAGRA [13] and LIGO-India [14] will join the aLIGO and AdV detectors to not only increase the detection rate but also improve the localization of GW sources - thereby, facilitating the search for their possible electromagnetic counterparts [15–17]. The global network of ground-based detectors will produce an unprecedentedly large amount of data, which will pose an interesting challenge by itself for GW data analysis.

At present, theoretically modeled compact binary coalescence (CBC) waveforms are used as templates to *matched-filter* [18] the detector data in GW searches for such astrophysical signals [19, 20]. The matched-filtering operation is implemented by cross-correlating the detector data with these templates. The template waveforms depend on a set of extrinsic parameters (e.g. the time  $t_0$  and phase  $\phi_0$  at arrival or coalescence of the signal in band), and intrinsic parameters (e.g., component masses and their spins). The matched-filter output  $\rho$ , is maximized over these parameters to get the optimal detection statistic and is often referred to as the signal-to-noise ratio (SNR). While  $\rho$  can be algebraically maximized over extrinsic parameters, it is evaluated over a large bank of templates constructed for a grid of values of the intrinsic parameters spanning astrophysical relevant ranges. A brute force implementation would be computationally expensive.

Several different grid placement algorithms have been

developed to minimize the required number of grid points [21–23]. As the aLIGO detectors are paced through the planned hardware upgrades, one expects better sensitivity at low frequencies and an increase in the the detector bandwidth. The seismic cutoff frequency is expected to decrease from 30 to 10 Hz. The combined effects of these changes will not only increase the volume of the search parameter space but also result in denser banks thereby increasing the redundancy in the template database. The improvement in low frequency response of the detector will also lead to more cycles of the GW signal to fall in band, thereby increasing the time duration of these signals. This highlights the need for designing efficient and scalable methods for matched-filtering-based templated compact binary coalescence (CBC) searches [24–29].

In a seminal work, Cannon *et al.* [30–32] have shown the efficacy of singular value decomposition (SVD) technique to address redundancies in the template bank. The attractiveness of this method stems from the fact that templates with similar parameter values are strongly correlated and its application to CBC searches effectively reduces the number of filters or templates with negligible effect on their performance. However, we shall show that the computational cost of SVD factorization does not scale favorably with increase in bank sizes. Further, it may not be possible to factorize very large banks *in toto* as it requires prohibitively large amount of random access memory.

Random Projections (RP), conceived by the pioneering work of Johnson and Lindenstrauss [33], is a computationally efficient technique for dimension reduction and finds applications in many areas of data science [34]. In this *Letter*, we apply this technique to address two key challenges in future CBC searches: handling redundancies in large template databases; and efficiently correlating noisy data against long templates.

The *primary impact* of this work is multi-fold: (1) Ef-

efficient template matrix factorization can be used to address the *redundancy problem*. This is similar in spirit to the SVD factorization that is at the heart of the “GstLAL”-based inspiral pipeline [29, 32, 35]. The RP-based method presented here scale well for very large number of templates embedded in high dimensional Euclidean space. In many scenarios such factorizations can be done off-line, in advance of a CBC search. Nonetheless there can be situations when the factors need to be updated on-line owing to the non-stationarity of data. Our adaptation of the method for CBC searches will benefit both scenarios. (2) We show the explicit connection between the new factorization scheme and the extant SVD method. This would not only bridge the two approaches but also make the new scheme readily usable. (3) The computational challenges arising from correlating noisy data against long templates (also known as the *curse of dimensionality*) is addressed by casting the matched-filtering operation itself in a lower-dimensional space. For certain types of template banks (e.g., for CBCs with precessing spins), the template matrix may be less amenable to a SVD-like factorization. In such cases, the total computational cost can be significantly reduced by using the RP-based correlation alone. (4) Finally, we show that RP-based template matrix factorization, on the one hand, and matched-filtering computation in reduced dimension, on the other, can be combined effectively for efficient CBC searches.

Currently the GstLAL-based inspiral pipeline utilizes time-slicing of templates to improve computational efficiency, and also involves spin-aligned templates. Since it is for the first time that the method of random projections is being introduced for gravitational wave searches, our primary objective here is to elucidate how its core ideas can help them. This is why we demonstrate application of RP in the simple case of a single slice of data and non-spinning inspiral templates. This simplification notwithstanding, the RP-based methods introduced here can be readily applied to time-sliced data and spin-aligned templates. (A detailed study of that application and the computational advantage so gained will be presented in a future work.)

**Compact binary searches.** Consider a CBC search involving a bank of  $N_T$  templates over a given parameter space. Following the convention in Ref. [30], let  $\mathbf{H}$  denote the  $2N_T \times N_s$  *template matrix* with  $2N_T$  rows of real-valued unit-norm whitened filters, each sampled over  $N_s$  time-points. The template matrix may be viewed as  $2N_T$  row-vectors embedded in  $N_s$ -dimensional Euclidean space  $\mathbb{R}^{N_s}$ . The complex matched-filter output of the  $\alpha^{\text{th}}$  template at a specific point in time, against the whitened data  $\vec{S}$  can be written as the inner product:

$$\rho_\alpha = (H_{(2\alpha-1)} - iH_{(2\alpha)}) \vec{S}^T, \quad (1)$$

where  $H_\alpha$  denotes the  $\alpha^{\text{th}}$  row of  $\mathbf{H}$  and  $\vec{S}^T$  is the transpose of  $\vec{S}$ . The signal-to-noise ratio maximized over the initial phase  $\phi_0$ , is given by  $|\rho_\alpha|$ . In our notation, the  $H_\alpha$ ’s and signal  $\vec{S}$  are assumed to be row vectors. The overlap between two templates, when maximized over *extrinsic* parameters produces the *match*. The match between templates with similar *intrinsic* parameters (such as the compact object masses), can be very high - sig-

nifying the rank deficiency of the template matrix. A typical *off-line* CBC search involves calculating the cross-correlation between  $\vec{S}$  and every row of  $\mathbf{H}$  for a series of relative time-shifts, or values of  $t_0$ , thereby generating a time-series of  $\rho_\alpha$  values, for every  $\alpha$ . The use of a large number of templates ( $N_T$ ), each sampled over a large number of points ( $N_s$ ) amplifies the computational cost in such a search model.

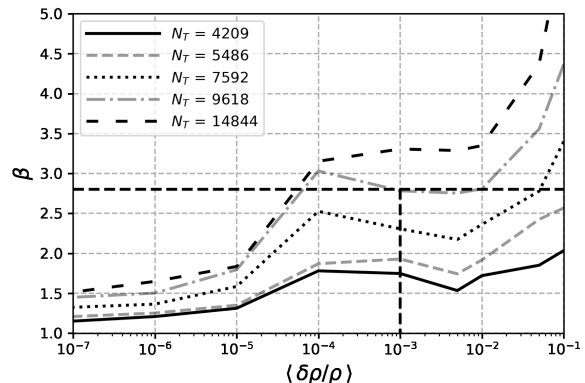


FIG. 1. The factor by which the number of SVD basis vectors increases due to partitioning of template bank of size  $N_T$  into sub-banks of 500 templates each is shown as  $\beta$  on the vertical axis. Results from five different template-bank sizes are shown. As one approaches machine-precision accuracy in SNR reconstruction,  $\beta \rightarrow 1$  as expected. A practical operating point would be  $\langle \delta\rho/\rho \rangle \sim 10^{-3}$ . The trend from the five examples shown here indicates that  $\beta$  can be quite large for searches in aLIGO data where  $N_T \sim 10^5$ .

The rank deficiency of  $\mathbf{H}$  is exploited in the truncated SVD approach, where every row is approximated as a linear combination of only  $\ell$  of the  $2N_T$  right singular vectors with the most dominant singular values. Further, these “basis” vectors are used as eigen-templates against which the data is cross-correlated. The left singular vectors of  $\mathbf{H}$  and the singular values are combined into a coefficient matrix that is used to reconstruct the approximate SNR. The truncation of the basis leads to errors in the approximation of the template waveforms, which further translates to imperfect reconstructions of the SNR. The fractional SNR loss can be measured as a function of the discarded  $(2N_T - \ell)$  singular values.

The SVD factorization of the template matrix  $\mathbf{H}$  has a time-complexity proportional to  $\mathcal{O}(N_T^2 N_s)$  assuming  $N_T \leq N_s$ . Thus, such factorizations fast become computationally unviable with increasing size of a template bank. Moreover, since the entire template matrix can become too large to be saved in single machine memory, a suitable parallel scheme is required to apply SVD to larger template banks. SVD-based on-line CBC searches [35, 36] work around this problem by splitting the bank into smaller sub-banks that are more amenable to such factorization separately. While the optimal way of partitioning the bank is an open problem, the act of splitting the bank prevents exploitation of the *linear dependency* of templates across the sub-banks. This is seen in Fig. 1, where we plot  $\beta$ , which is defined as the ratio of the number of basis vectors summed across all the sub-banks to the number of basis vectors from the

SVD factorization of the full bank, at a given average fractional loss in accuracy of the reconstructed SNR. It is clear that by splitting the bank, one effectively ends up requiring many more eigen-templates against which the data is filtered.

The SVD-inspired RP based template matrix factorization presented in the following sections of this *Letter* addresses this issue and is scalable for large template banks. We also apply RP to calculate the correlations in a lower dimensional space  $\mathbb{R}^k$  where  $k \leq N_s$ . These correlations could be either between a template and the data as shown in Eq. (1) or between the basis vectors and the data within the SVD paradigm. The full potential of the RP-based methods introduced here can be realized by combining them together. We demonstrate its feasibility with an example.

**Random projection.** The core theoretical idea behind the Random Projection (RP) technique is the Johnson-Lindenstrauss (JL) lemma [33], which states that a set of  $2N_T$  vectors in  $\mathbb{R}^{N_s}$  can be mapped into a randomly generated subspace  $\mathbb{R}^k$  of dimension  $k \sim \mathcal{O}(\log 2N_T / \epsilon^2)$  while preserving all pairwise  $L_2$  norms to within a factor of  $(1 \pm \epsilon)$ , where  $0 < \epsilon < 1$ , with a very high probability. Here,  $\epsilon$  is the mismatch or distortion tolerated in the pairwise  $L_2$  norms between any two filters after projection. Thus, RP also approximately preserves any statistic of the dataset that is characterized by such pairwise distances. The RP of  $\mathbf{H}$  onto  $\mathbb{R}^k$  produces  $\mathbf{H}\mathbf{\Omega}$ ; in this data-oblivious transformation, the accuracy of the transformation depends on the target dimensions and sampling distribution of the  $N_s \times k$  projection matrix  $\mathbf{\Omega}$ . While it is enough to sample the entries independently and identically distributed from a sub-Gaussian distribution, here we choose them independently from a Gaussian distribution with mean zero and variance  $1/k$ , i.e.,  $\mathcal{N}(0, 1/k)$ , thus producing a Gaussian quasi-orthonormal random matrix [37, 38] such that  $\langle \mathbf{\Omega}\mathbf{\Omega}^T \rangle = \mathbf{I}$ . Results obtained from RP-based processing can vary based on the actual choice of the distribution (from which elements of  $\mathbf{\Omega}$  are drawn), and in a statistical sense, these results arising from different choices of  $\mathbf{\Omega}$  are expected to be equivalent due to the quasi-orthonormality of the projection, as explained intuitively in the Supplemental Material.

**RP-based template matrix factorization.** The key idea behind an  $\ell$ -truncated SVD approximation of  $\mathbf{H}$  is to reconstruct the rows of the template matrix using the top- $\ell$  right singular vectors. This approximation works well since  $\mathbf{H}$  has a fast-decaying spectrum, as shown in Fig. 2. In making the truncation, one effectively reduces  $\mathbf{H}$  to its  $\ell$ -rank approximation  $\mathbf{H}^{(\ell)}$ . Further, for a bank of normalized templates, it is easy to show that the average fractional loss in SNR due to the truncation is given as  $\langle \delta\rho/\rho \rangle = \|\mathbf{H} - \mathbf{H}^{(\ell)}\|_F^2 / \|\mathbf{H}\|_F^2$ , where  $\|\cdot\|_F$  denotes the Frobenius norm [39]. However, the existing SVD algorithms do not scale well with increasing dimensions and redundancies of the template database.

Randomized-SVD (RSVD) [40] is a RP-based matrix-factorization technique to obtain an  $\ell$ -rank matrix factorization  $\mathbf{H}^{(\ell)}$  such that, for some specified  $\eta > 0$ ,  $\|\mathbf{H} - \mathbf{H}^{(\ell)}\|_F \leq \min_{\{\mathbf{X} : \text{rank}(\mathbf{X}) \leq \ell\}} \|\mathbf{H} - \mathbf{X}\|_F (1 + \eta)$  with high probability. The RSVD algorithm proceeds by first

projecting the individual row-vectors in the template matrix  $\mathbf{H}$  to  $\mathbb{R}^\ell$  by using  $\tilde{\mathbf{\Omega}}_{N_s \times \ell} \in \mathcal{N}(0, 1/\ell)$ , thereby yielding  $\tilde{\mathbf{H}}_{2N_T \times \ell} = \mathbf{H}\tilde{\mathbf{\Omega}}$ . The latter can be used to perform an SVD-like factorization directly in  $\mathbb{R}^\ell$  through a series of operations as described below.

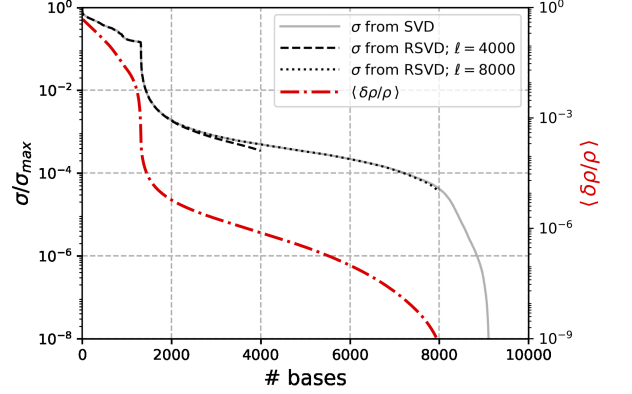


FIG. 2. Left vertical-axis: Comparison of singular values  $\sigma$  of the template matrix of size  $9130 \times 65536$  (normalized by the maximum singular value  $\sigma_{max}$ ) as obtained from SVD and RSVD factorization. RSVD is performed in target dimensions  $\mathbb{R}^\ell$  where  $\ell = 4000$  or  $8000$ . The spectrum is seen to fall steeply. Right vertical axis: Average SNR reconstruction error as given in Eq. (3) for  $\ell = 8000$ . As expected, the reconstruction improves with increasing number of basis vectors.

As seen in Fig. 2, it is typically sufficient to take  $\ell \ll N_T$ . In fact, the numerical value of  $\ell$  chosen in RSVD might be smaller than the theoretical JL bound prescribed for preserving pairwise  $L_2$  distances between the  $2N_T$  rows to a  $\eta$  distortion factor. Working with the reduced sized matrix  $\tilde{\mathbf{H}}$  leads to significant computational savings, while producing a decomposition that closely approximates the optimal  $\ell$ -rank factorization of  $\mathbf{H}$ . It is customary to oversample  $\ell$  by a small factor for better numerical results. This is implicitly assumed in the following discussions.

RSVD thus proceeds by obtaining a set of orthogonal bases for the column space of  $\tilde{\mathbf{H}}$  by using a QR decomposition:  $\tilde{\mathbf{H}} = \mathbf{Q}\mathbf{R}$ , where  $\mathbf{Q}$  is an orthonormal matrix with dimensions  $2N_T \times \ell$ . The approximate rank- $\ell$  decomposition is then obtained as  $\mathbf{H}^{(\ell)} = \mathbf{Q}(\mathbf{Q}^T\mathbf{H}) = \mathbf{Q}\mathbf{B}$ , where  $\mathbf{B}_{\ell \times N_s} \equiv \mathbf{Q}^T\mathbf{H}$  is a matrix that defines the orthonormal projection of the template waveforms into the compressed subspace.

From the factorization of  $\mathbf{H}$  as shown above, it is clear that one can use the  $\ell$  rows of  $\mathbf{B}$  as the surrogate templates, which in turn can be used to correlate against the detector data  $\tilde{\mathbf{S}}$  in GW searches. These can be further combined with  $\mathbf{Q}$  to reconstruct  $\rho$  in  $\mathbb{R}^{N_s}$ . We can thus use the QB decomposition itself, as described above, to improve the efficiency of both the time and frequency domain searches by constructing  $\mathbf{H}$  appropriately, with templates from the corresponding domains.

Instead of randomly projecting the column space of  $\mathbf{H}$ , the method can be generalized by applying RP on both the row and column spaces [40]. This bilateral RSVD method is particularly useful when both  $N_s$  and  $N_T$  are very large. Figure 2 compares the singular values



obtained by the RP-based factorization against those from a direct SVD factorization.

**Reconstruction of SNR.** The rank- $\ell$  matrix factorization of  $\mathbf{H}$  using RSVD is given by  $\mathbf{H}^{(\ell)} = \mathbf{Q}\mathbf{B}$ . Thus, the SNR  $\rho'_\alpha$ , for any given  $t_0$ , can be reconstructed in  $\mathbb{R}^{N_s}$  as

$$\begin{aligned} \rho'_\alpha &= \left( H_{(2\alpha-1)}^{(\ell)} - iH_{(2\alpha)}^{(\ell)} \right) \bar{S}^T \\ &= \sum_{\nu=1}^{\ell} \left( Q_{(2\alpha-1)\nu} - iQ_{(2\alpha)\nu} \right) \left( B_\nu \bar{S}^T \right). \end{aligned} \quad (2)$$

Using Pythagoras theorem, and the fact that  $\|\mathbf{H}\|_F^2 = 2N_T$ , it is easy to show that the average fractional loss of SNR is given by

$$\left\langle \frac{\delta\rho}{\rho} \right\rangle \leq \frac{\|\mathbf{H}\|_F^2 - \|\mathbf{H}^{(\ell)}\|_F^2}{\|\mathbf{H}\|_F^2} = 1 - \frac{\sum_{\mu=1}^{\ell} \sigma_\mu^2}{2N_T}, \quad (3)$$

where  $\langle \rangle$  denotes average over the bank of templates and the  $\sigma_\mu$  are the eigenvalues of  $\mathbf{H}^{(\ell)}$ . For the example discussed in Fig. 2,  $\sum_{\mu=1}^{\ell} \sigma_\mu^2 / (2N_T)$  is smaller than unity, but approaches it monotonically with increasing  $\ell$ . The right-hand side of Eq. (2) can be calculated efficiently by evaluating the Frobenius norm of  $\mathbf{B}$  directly (i.e., without explicitly finding the eigenvalues of  $\mathbf{H}^{(\ell)}$  first). Thus, the QB decomposition can indeed serve as a stand-in replacement for the SVD factorization.

An efficient method of explicitly calculating the SVD factors from the RP-based factorization is now presented. This is intended as a bridge between the two methods. Singular values can be obtained by performing an SVD on  $\mathbf{B}$ , or by first calculating  $\mathbf{T}_B = \mathbf{B}\mathbf{B}^T$ , of size  $\ell \times \ell$ . The eigenvectors  $\mathbf{U}_{T_B}$  of  $\mathbf{T}_B$  are identical to the left singular vectors of  $\mathbf{B}$ , and the eigenvalues  $\Sigma_{T_B}$  are equal to the squares of the singular values of  $\mathbf{B}$ . As  $\mathbf{T}_B$  is a much more compressed matrix compared to  $\mathbf{B}$ , it is far more efficient to store it in memory and factorize it thereby revealing the singular values and left singular vectors. These in turn can be further used to calculate the singular values of  $\mathbf{H}^{(\ell)}$ . The top- $\ell$  right singular vectors of  $\mathbf{H}$  in  $\mathbb{R}^{N_s}$  can be obtained using the left singular vectors of  $\mathbf{T}_B$ :  $\mathbf{U}_H^{(\ell)} \approx \mathbf{Q}\mathbf{U}_{T_B}$ . Similarly, it can be trivially checked that  $\Sigma_H \mathbf{V}_H^T = \mathbf{U}_{T_B}^T \mathbf{B}$ . Thus, all the pieces of the SVD factorization of  $\mathbf{H}$  can be recovered from RSVD factors, but at a small fraction of the computational cost of the former. In doing so, the advantages of RP-based factorization can be directly transferred to the current SVD based data analysis pipelines.

Ideally one would like to use  $\langle \delta\rho/\rho \rangle$  as the control parameter and solve Eq. (3) for the optimum value of  $\ell$ . However, this is a hard problem and in practice the value is set by a process of trial and error, which thankfully can be done off-line even when the computation in Eq. (2) is conducted on-line.

**Random projection based correlations.** A naive implementation of matched-filter in time-domain can be very expensive, with a complexity of  $\mathcal{O}(N_s^2)$  per template. In this section we show how random projections can be applied to reduce this cost considerably: the two aforementioned whitened time-series vectors in  $\mathbb{R}^{N_s}$  can be first projected to a random  $k$ -dimensional ( $k \ll N_s$ )

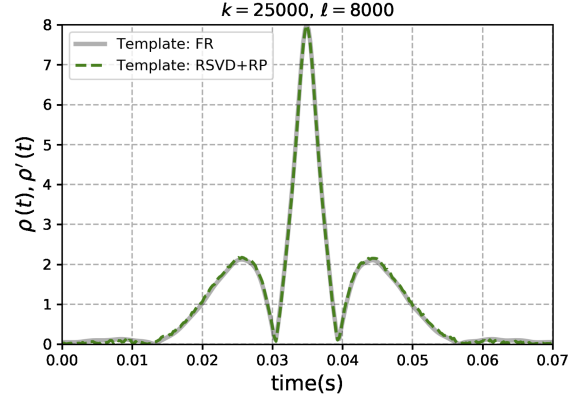


FIG. 3. The SNR time series obtained by calculating the direct correlation of  $\tilde{S}$  against a template in  $\mathbb{R}^{N_s}$  (solid line) where  $N_s = 221\,184$  is compared to the reconstructed time series (dashed line) using a combination of both the RP based methods presented here. In the latter case, the template matrix of  $N_T = 15\,870$  rows is at first RSVD factorized for  $\ell = 8000$ . Thereafter, correlations with  $\tilde{S}$  are calculated in the target space  $\mathbb{R}^k$  for  $k = 25\,000$ . The peak reconstruction error in this case is  $4 \times 10^{-3}$  and comes from a combination of both the approximations used. The component mass parameters of the injected signal ( $m_1 = 8.41 M_\odot, m_2 = 1.7 M_\odot$ ) are chosen to be the same as one of the templates in the bank. The distortion factor on SNR from the JL-lemma is  $\epsilon = 0.1$ .

subspace and then cross-correlated; the pairwise distance-preserving property of RP guarantees that the matched-filter output  $\rho'_\alpha$  in  $\mathbb{R}^k$  will be approximately equal to  $\rho_\alpha$  in  $\mathbb{R}^{N_s}$ , i.e.

$$\begin{aligned} \langle \rho'_\alpha \rangle &= \langle (H_{(2\alpha-1)} \Omega - iH_{(2\alpha)} \Omega) (\tilde{S} \Omega)^T \rangle \\ &= \langle (H_{(2\alpha-1)} \Omega \Omega^T - iH_{(2\alpha)} \Omega \Omega^T) \tilde{S}^T \rangle \\ &= \rho_\alpha, \end{aligned} \quad (4)$$

where we have used  $\langle \Omega \Omega^T \rangle = I$  (by construction).

It can also help searches to use the RP-based correlation in conjunction with the RP-based QB factorization of the template matrix described above. The key to this fusion between the two RP-based methods lies in the fact that instead of matched-filtering the data  $\tilde{S}$  against every template in the bank, one can use the reduced set of  $\ell \leq 2N_T$  row vectors of  $\mathbf{B}$  as surrogate templates for this purpose. These correlations can be calculated in  $\mathbb{R}^k$  by projecting  $\tilde{S}$  and each row vector  $B_\nu \in \mathbb{R}^{N_s}$  to the target  $k$ -dimensional subspace. Such projections preserve the inner products between the data and  $B_\nu$  at every relative time-shift within the  $\epsilon$  bound, as guaranteed by the JL lemma. The complex SNR for each template can be reconstructed using the coefficient matrix  $\mathcal{C}_{N_T \times \ell}$ , whose elements are  $\mathcal{C}_\alpha \equiv (Q_{(2\alpha-1)\nu} - iQ_{(2\alpha)\nu})$  as shown in Eq. (2). The phase-maximized SNRs of the templates are given by the modulus of resulting complex SNRs.

The construction proceeds as follows: Suppose data are sampled at a rate  $f_s$  and that the duration in which one decides to search for the signal's time of arrival is  $\tau$ , which is taken to be longer than the longest template in the bank. Then the number of points over which one is discretely searching for  $t_0$  is  $f_s \tau$ . We next construct a partial circulant matrix  $\mathbf{K}(B_\nu)$  for every row of  $\mathbf{B}$ , such that its dimensions are  $(f_s \tau) \times (f_s \tau + N_s)$ . Its  $n^{\text{th}}$  row

$K_n(B_\nu)$  is a copy of  $B_\nu$  that is time-shifted by an amount  $\Delta t_n = n/f_s$ , where  $n \in [0, (f_s\tau)]$ . The remaining  $f_s\tau$  elements in each row are set to zero. The data vector  $\vec{S}$ , with  $(f_s\tau + N_s)$  time-points, and the circulant matrices can both be randomly projected to the subspace  $\mathbb{R}^k$  using  $\Omega$ . Their subsequent multiplication is used to construct the cross-correlation:

$$\rho'_\alpha(\Delta t_n) = \sum_\nu \mathcal{C}_{\alpha\nu} (K_n(B_\nu) \Omega) (\vec{S}\Omega)^T, \quad (5)$$

where  $\alpha$  is the index over the templates in the bank  $\nu = 1, \dots, \ell$  is the index on the rows of  $\mathbf{B}$ , and  $\Omega$  has dimensions of  $(f_s\tau + N_s) \times \ell$ . A circulant matrix can be diagonalized using FFT-like algorithms to enable efficient processing of matrix-vector products involving such matrices [39].

The efficacy of the above construction is demonstrated in Fig. 3 by the help of a simple example, where the SNR time series  $\rho(t)$  calculated by directly correlating the data against the “exactly-matched” template in  $\mathbb{R}^{N_s}$  is compared against the SNR time series  $\rho'(t)$  reconstructed using the RP-based techniques proposed in this work. A template bank consisting of  $N_T = 15870$  templates was used for this demonstration with component masses between  $(1.5 - 15) M_\odot$ . The data time series consists of a simulated CBC signal with component masses  $m_1 = 8.41 M_\odot$  and  $m_2 = 1.7 M_\odot$  chosen to coincide with one of the templates in the bank. For simplicity, no noise was added to this data snippet. The data and template time-series were sampled over  $N_s = 221184$  points. The template matrix  $\mathbf{H}$  was at first reduced to its  $\ell = 8000$  rank approximation and RP-factorized. All the rows of  $\mathbf{B}$  were used as surrogate templates to correlate the data in a target dimension of  $\mathbb{R}^k$  where  $k = 25000$ . These were then further combined with the corresponding row of the coefficient matrix  $\mathbf{C}$  to reconstruct the SNR time series. For the choice of  $\ell$  and  $k$  used in this example, we see a good agreement between the two SNR time series, with a negligible fractional peak reconstruction error of  $\sim 10^{-4}$ . The loss in SNR arises from both the RP based techniques used here i.e. from approximating the template matrix by  $\mathbf{H}^{(\ell)}$ , as well as from projecting the data and template surrogates to the lower  $k$ -dimensional target space for carrying out the correlation. The optimal choice of  $\ell$  and  $k$  can be made by balancing the reconstruction errors against the desired computational speed-up.

**Computational complexity analysis.** The straightforward SVD factorization of  $\mathbf{H}$  requires  $\mathcal{O}(N_T^2 N_s)$  floating-point operations, assuming  $N_T \leq N_s$ . In comparison, the cost of the RP matrix factorization is  $\mathcal{O}(\ell N_T N_s + (\ell^2 N_T - \frac{2}{3}\ell^3) + \ell N_T N_s + \ell N_s)$ . In this last expression, we have included partial contributions from first projecting the template matrix to  $\mathbb{R}^\ell$ , then taking the QR decomposition of  $\tilde{\mathbf{H}}$  using Householder’s method [41], followed by the cost of constructing  $\mathbf{B}$  and calculating its Frobenius norm. For practical cases, one expects  $\ell \ll N_s$ , due to which the cost of factorizing  $\mathbf{H}$  can be several orders of magnitude less than a full SVD factorization. This advantage is not just realized off-line, but can also directly impact the total on-line cost of the searches owing a lower value of  $\ell$  alone: Figure 1

shows that for moderate sized banks one effectively ends up using  $\sim 3 - 4$  times fewer surrogate templates in the on-line portion of the search from the new RP-based factorization. This improvement is expected to be higher for larger banks.

For on-line searches, the number of floating point operations per second (flops) in our method is  $N_{\text{flops}} = (2\ell k f_s + 2\ell N_T f_s + k f_s)$ . The first term is the number of floating-point operations required for computing the cross-correlation between the surrogate templates (rows of  $\mathbf{B}$ ) and the data vector; the second term is the cost of reconstruction of the SNR for every template; and the third term is the cost of projecting the data vector into the lower-dimensional space. In the SVD-only method, the expression for  $N_{\text{flops}}$  is analogous, except that instead of the last term above, it has a down-sampling cost that is similarly insignificant as our projection cost. The primary difference between the two methods is that owing to our use of RSVD and RP,  $\ell$  and  $k$  are less than the number of basis templates and the number of time samples of data used, respectively, in the SVD-only method. For the crucial last couple of seconds of the cross-correlation analysis for CBC signals we have evaluated that our method is an order of magnitude faster than the SVD-only method.

**Summary of results.** We have proposed a new, computationally efficient random projection based technique to factorize the template matrix. This method is scalable to very large template banks expected in the compact binary GW searches in aLIGO era. The simple atomic matrix operations required in the factorization makes it easily parallelizable over a distributed architecture. We have also showed how the computation of the matched-filter can be sped up by using RP on both the filters and the data and computing their cross-correlation in the target lower-dimension space. The search over the time-of-arrival of the signal is facilitated by the use of circulant matrices. Finally, we argue that the two methods can be combined very effectively to reduce the total computational cost by an order of magnitude in comparison to a baseline search where the template matrix is SVD factorized and correlations are calculated in  $\mathbb{R}^{N_s}$ . These new techniques may help to reduce the computational footprint of on-line CBC searches, thereby freeing up resources for more complex searches, e.g., for CBCs with generic spins and, hence, improving the chances for new discoveries.

**Acknowledgments.** We would like to thank Surabhi Sachdev for carefully reading the manuscript and making useful comments. This work is supported in part by DST’s SERB and ICPS programs, NSF grant PHY-1506497, and the Navajbai Ratan Tata Trust.

- 
- [1] J. Aasi *et al.* (LIGO Scientific), *Class. Quant. Grav.* **32**, 074001 (2015), [arXiv:1411.4547 \[gr-qc\]](#).
  - [2] B. P. Abbott *et al.* (Virgo, LIGO Scientific), *Phys. Rev. Lett.* **116**, 061102 (2016), [arXiv:1602.03837 \[gr-qc\]](#).
  - [3] B. P. Abbott *et al.* (Virgo, LIGO Scientific), *Phys. Rev. Lett.* **116**, 241103 (2016), [arXiv:1606.04855 \[gr-qc\]](#).
  - [4] B. P. Abbott *et al.* (Virgo, LIGO Scientific), *Phys. Rev.*

- X6**, 041015 (2016), arXiv:1606.04856 [gr-qc].
- [5] B. P. Abbott *et al.* (VIRGO, LIGO Scientific), *Phys. Rev. Lett.* **118**, 221101 (2017), arXiv:1706.01812 [gr-qc].
- [6] B. P. Abbott *et al.* (Virgo, LIGO Scientific), *Phys. Rev. Lett.* **119**, 141101 (2017), arXiv:1709.09660 [gr-qc].
- [7] F. Acernese *et al.* (VIRGO), *Class. Quant. Grav.* **32**, 024001 (2015), arXiv:1408.3978 [gr-qc].
- [8] B. P. Abbott *et al.* (Virgo, LIGO Scientific), *Phys. Rev. Lett.* **119**, 141101 (2017), arXiv:1709.09660 [gr-qc].
- [9] B. P. Abbott *et al.* (Virgo, LIGO Scientific), (2017), arXiv:1711.05578 [astro-ph.HE].
- [10] B. P. Abbott *et al.* (Virgo, LIGO Scientific), *Phys. Rev. Lett.* **119**, 161101 (2017), arXiv:1710.05832 [gr-qc].
- [11] B. P. Abbott *et al.* (Virgo, Fermi-GBM, INTEGRAL, LIGO Scientific), *Astrophys. J.* **848**, L13 (2017), arXiv:1710.05834 [astro-ph.HE].
- [12] B. P. Abbott *et al.*, *Astrophys. J.* **848**, L 12 (2017), arXiv:1710.05833.
- [13] T. Akutsu *et al.* (KAGRA) (2017) arXiv:1710.04823 [gr-qc].
- [14] C. S. Unnikrishnan, *Int. J. Mod. Phys. D* **22**, 1341010 (2013), arXiv:1510.06059 [physics.ins-det].
- [15] J. Rana, A. Singhal, B. Gadre, V. Bhalerao, and S. Bose, *Astrophys. J.* **838**, 108 (2017), arXiv:1603.01689 [astro-ph.IM].
- [16] V. Srivastava, V. Bhalerao, A. P. Ravi, A. Ghosh, and S. Bose, *Astrophys. J.* **838**, 46 (2017), arXiv:1610.07154 [astro-ph.HE].
- [17] S. Ghosh and S. Bose, (2013), arXiv:1308.6081 [astro-ph.HE].
- [18] C. W. Helstrom, *Elements of Signal Detection and Estimation* (Prentice-Hall, Inc., Upper Saddle River, NJ, USA, 1995).
- [19] B. J. Owen, *Phys. Rev. D* **53**, 6749 (1996), arXiv:gr-qc/9511032 [gr-qc].
- [20] B. S. Sathyaprakash and S. V. Dhurandhar, *Phys. Rev. D* **44**, 3819 (1991).
- [21] R. Prix, *Gravitational wave data analysis. Proceedings: 11th Workshop, GWDAA-11, Potsdam, Germany, Dec 18-21, 2006*, *Class. Quant. Grav.* **24**, S481 (2007), arXiv:0707.0428 [gr-qc].
- [22] I. W. Harry, B. Allen, and B. S. Sathyaprakash, *Phys. Rev. D* **80**, 104014 (2009), arXiv:0908.2090 [gr-qc].
- [23] S. Roy, A. S. Sengupta, and N. Thakor, *Phys. Rev. D* **95**, 104045 (2017), arXiv:1702.06771 [gr-qc].
- [24] T. Cokelaer, *Phys. Rev. D* **76**, 102004 (2007), arXiv:0706.4437 [gr-qc].
- [25] B. Abbott *et al.* (LIGO Scientific), *Phys. Rev. D* **78**, 042002 (2008), arXiv:0712.2050 [gr-qc].
- [26] I. W. Harry, A. H. Nitz, D. A. Brown, A. P. Lundgren, E. Ochsner, and D. Keppel, *Phys. Rev. D* **89**, 024010 (2014), arXiv:1307.3562 [gr-qc].
- [27] S. Babak, *Class. Quant. Grav.* **25**, 195011 (2008), arXiv:0801.4070 [gr-qc].
- [28] G. M. Manca and M. Vallisneri, *Phys. Rev. D* **81**, 024004 (2010), arXiv:0909.0563 [gr-qc].
- [29] S. Privitera, S. R. P. Mohapatra, P. Ajith, K. Cannon, N. Fotopoulos, M. A. Frei, C. Hanna, A. J. Weinstein, and J. T. Whelan, *Phys. Rev. D* **89**, 024003 (2014), arXiv:1310.5633 [gr-qc].
- [30] K. Cannon, A. Chapman, C. Hanna, D. Keppel, A. C. Searle, and A. J. Weinstein, *Phys. Rev. D* **82**, 044025 (2010), arXiv:1005.0012 [gr-qc].
- [31] K. Cannon, C. Hanna, and D. Keppel, *Phys. Rev. D* **84**, 084003 (2011), arXiv:1101.4939 [gr-qc].
- [32] K. Cannon *et al.*, *Astrophys. J.* **748**, 136 (2012), arXiv:1107.2665 [astro-ph.IM].
- [33] W. B. Johnson and J. Lindenstrauss, in *Conference in modern analysis and probability (New Haven, Conn., 1982)*, Contemp. Math., Vol. 26 (Amer. Math. Soc., Providence, RI, 1984) pp. 189–206.
- [34] E. Bingham and H. Mannila, in *Proceedings of the seventh ACM SIGKDD international conference on Knowledge discovery and data mining* (ACM, 2001) pp. 245–250.
- [35] C. Messick *et al.*, *Phys. Rev. D* **95**, 042001 (2017), arXiv:1604.04324 [astro-ph.IM].
- [36] K. Cannon *et al.*, *Astrophys. J.* **748**, 136 (2012), arXiv:1107.2665 [astro-ph.IM].
- [37] S. Dasgupta and A. Gupta, *Random Struct. Algorithms* **22**, 60 (2003).
- [38] S. Dasgupta, in *Proceedings of the Sixteenth conference on Uncertainty in artificial intelligence* (Morgan Kaufmann Publishers Inc., 2000) pp. 143–151, arXiv:1301.3849 [cs.LG].
- [39] G. H. Golub and C. F. Van Loan, *Matrix Computations (3rd Ed.)* (Johns Hopkins University Press, Baltimore, MD, USA, 1996).
- [40] N. Halko, P.-G. Martinsson, and J. A. Tropp, *SIAM review* **53**, 217 (2011), arXiv:0909.4061 [math.NA].
- [41] W. H. Press, S. A. Teukolsky, W. T. Vetterling, and B. P. Flannery, *Numerical Recipes 3rd Edition: The Art of Scientific Computing*, 3rd ed. (Cambridge University Press, New York, NY, USA, 2007).

## SUPPLEMENTAL MATERIAL

The purpose of this Appendix is to describe the geometric intuition behind the claim that RSVD preserves the top singular subspaces. Figure 4 depicts this intuition. We denote the  $L_2$  norm of a vector as  $\|\cdot\|$ . Recall that given  $\mathbf{H}$ , finding out the top- $k$  singular vectors is akin to the question of finding out orthogonal directions  $u_1, \dots, u_k$  such that if  $\mathbf{U} = [u_1, \dots, u_k]$ , then  $\|\mathbf{U}\mathbf{U}^T\mathbf{H}\|_F^2 = \|\mathbf{U}^T\mathbf{H}\|_F^2 = \sum_{i=1}^k \|u_i^T\mathbf{H}\|^2$  is maximized (squared lengths of vectors in subfigure (a)).

Given the length-preserving properties of random projection, the sum of the squared lengths of  $u_i^T\mathbf{H}$  is equivalent, up to an approximation factor of  $1 \pm \epsilon$ , to the sum of squared lengths of  $(u_i^T\mathbf{H})\mathbf{\Omega}$  ((subfigure (b)), i.e.,

$$(1 - \epsilon) \sum_{i \leq k} \|u_i^T\mathbf{H}\|^2 \leq \sum_{i \leq k} \|(u_i^T\mathbf{H})\mathbf{\Omega}\|^2.$$

Hence, we instead find orthonormal vectors  $\{a_1, \dots, a_k\}$ , the top- $k$  left singular directions of  $\mathbf{H}\mathbf{\Omega}$ , such that  $\sum_{i \leq k} \|a_i^T(\mathbf{H}\mathbf{\Omega})\|^2$  is maximum (subfigure (c)), thus achieving  $\sum_{i \leq k} \|a_i^T(\mathbf{H}\mathbf{\Omega})\|^2 \geq \sum_{i \leq k} \|u_i^T(\mathbf{H}\mathbf{\Omega})\|^2$ .

Again by using the length preservation of random projection, we have that  $\|a_i^T\mathbf{H}\|^2 \geq (1 - \epsilon)\|(a_i^T\mathbf{H})\mathbf{\Omega}\|^2$  (subfigure

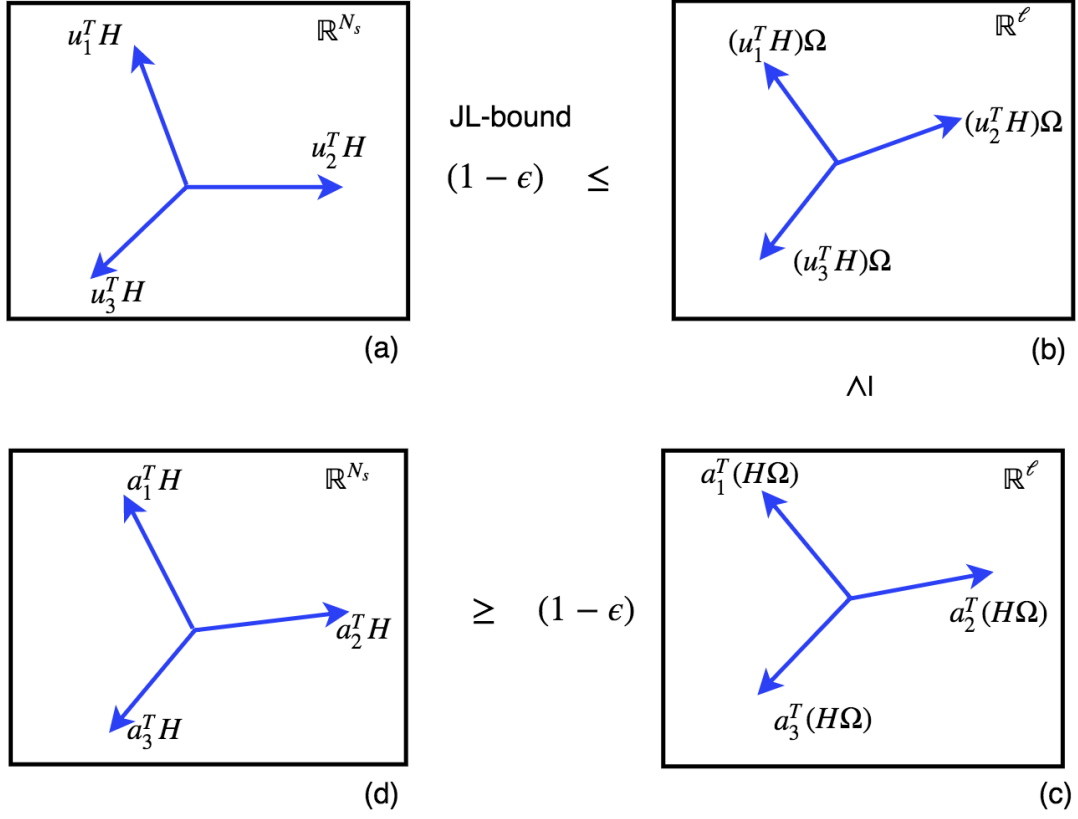


FIG. 4. Depiction of the geometrical intuition behind the preservation of the top singular subspaces in RSVD. Finding the top- $k$  singular vectors for a given  $\mathbf{H}$  is akin to the finding the orthogonal directions  $u_1, \dots, u_k$  such that the sum of lengths of the vectors  $u_i^T \mathbf{H}$  is maximized. Subfigure (a) shows these vectors in the original feature space. Subfigure (b) depicts the action of random projection of these vectors to a lower-dimensional space using the projection matrix  $\Omega$ . The length-preserving properties of random projections guarantee that the distortion in their lengths lies within a factor of  $1 \pm \epsilon$ . Subfigure (c) depicts the action of  $\mathbf{H}\Omega$  along its top- $k$  left singular directions  $\{a_1, \dots, a_k\}$ , such that  $\sum_{i \leq k} \|a_i^T(\mathbf{H}\Omega)\|^2$  is maximum. Note that these vectors  $a_i^T(\mathbf{H}\Omega)$ , can also be geometrically interpreted as the random projection of the vectors  $a_i^T \mathbf{H}$  (as shown in Subfigure (d)) using  $\Omega$ . Through this chain of subfigures, it follows that the low rank approximation  $\mathbf{A}\mathbf{A}^T \mathbf{H}$  found by RSVD captures most of the energy in the optimal rank- $k$  approximation  $\mathbf{U}\mathbf{U}^T \mathbf{H}$ .

(d)). Putting the above steps together, we find

$$\sum_{i=1}^k \|a_i^T \mathbf{H}\|^2 \geq (1 - \epsilon) \sum_{i=1}^k \|(a_i^T \mathbf{H})\Omega\|^2 \geq (1 - \epsilon) \sum_{i=1}^k \|(u_i^T \mathbf{H})\Omega\|^2 \geq (1 - \epsilon)^2 \sum_{i=1}^k \|(u_i^T \mathbf{H})\|^2.$$

Recall that by definition of singular vectors, we already have  $\sum_{i=1}^k \|a_i^T \mathbf{H}\|^2 \leq \sum_{i=1}^k \|u_i^T \mathbf{H}\|^2$ . Let  $\mathbf{A} = [a_1, \dots, a_k]$  and recall that  $\mathbf{U} = [u_1, \dots, u_k]$ . Given that  $\mathbf{U}$  is an orthonormal matrix, the matrix  $\mathbf{U}\mathbf{U}^T \mathbf{H}$  represents the projection of columns of  $\mathbf{H}$  onto the subspace spanned by the columns of  $\mathbf{U}$ , and hence is a rank- $k$  approximation of  $\mathbf{H}$ . Therefore, it follows from the above argument, that the low rank approximation  $\mathbf{A}\mathbf{A}^T \mathbf{H}$  found by RSVD captures most of the energy in the optimal rank- $k$  approximation  $\mathbf{U}\mathbf{U}^T \mathbf{H}$ .